Building Tomorrow's Society

Bâtir la Société de Demain

Fredericton, Canada

June 13 – June 16, 2018/ *Juin 13 – Juin 16, 2018*

ALTERATION OF WIND LOAD ON TALL BUILDINGS DUE TO FLUID STRUCTURE INTERACTION

Elshaer, Ahmed[1,3], Bitsuamlak, Girma[1,4], El Ansary, Ayman[2] and Sobhy, Masoud[3]
[1] Western University, Canada
[2] Stephenson Engineering, Canada
[3] aelshae@uwo.ca
[4] gbitsuam@uwo.ca

Abstract: Since wind is a governing design load for various structures, an accurate simulation of the aerodynamics will reduce the uncertainty associated with wind load evaluation on structures, and consequently their cost. Thus, highly accurate and reliable computational fluid dynamics (CFD) modeling is required to simulate and evaluate the wind behaviour for wind-induced loads. The state-of-the-art in numerical modeling of wind-structure interaction of a tall building is usually conducted by simulating structures as rigid bodies, then accounting for the dynamic effect throughout subsequent dynamic analyses. However, this can be considered a rigorous assumption when dealing with flexible structures (e.g. slender tall buildings and long span bridges), because the structure's motion may alter the wind flow field leading to changes in the resulting wind loads on the structure. The proper modeling for flexible structures, considering wind-structure interaction, requires the allowance of structures to vibrate within the wind flow that is simulated numerically by CFD analysis, namely "aero-elastic modeling". The current study uses an equivalent solid model that can simulate the structural behaviour of a detailed skeletal model during wind events. The study also highlights the importance of considering the fluid-structure interaction for tall buildings with high flexibility and demonstrates the possible wind load variation with different flexibility levels.

1 INTRODUCTION

Nowadays, Computational Fluid Dynamics (CFD) analysis is being adopted in many engineering applications, such as natural ventilation (Ding et al. 2005; van Hooff et al. 2011), pollution dispersion (Chu et al. 2005; Gousseau et al. 2011; Pospisil et al. 2004), assessment of thermal comfort (Catalina et al. 2009; Tablada et al. 2009), and wind speed comfort (Adamek et al. 2017; Blocken and Stathopoulos 2013). CFD was also adopted in studying wind-induced load on various structures including low-rise (Hajra et al. 2016; Yang et al. 2008), tall buildings (Aboshosha et al. 2015; Dagnew and Bitsuamlak 2014, 2012), bridges (Lee et al. 1997), and solar panels (Bitsuamlak et al. 2010). The continuous development in computational power and simulation techniques encouraged the use of CFD to explore fields where experimental modelling is difficult, expensive or time consuming, such as in design optimization (Bernardini et al. 2015; Elshaer et al. 2016b) and city scale assessment (Elshaer et al. 2017; Montazeri and Blocken 2013).

Numerical simulation of wind flow and its interaction with tall buildings is a complex process. The complexity arises due to many factors including: (i) modelling the incoming wind characteristics (e.g. wind speed,

turbulence, and correlations), (ii) accounting for the exposure and the surrounding conditions, and (iii) the interaction between wind and building(s). The latter factor is typically tackled, in both experimental and numerical simulation of wind flow, by only considering the flow aerodynamics (i.e. assuming the building to be a rigid body), while the dynamic effect of wind load is performed subsequent to the wind simulation process. This assumption could only be applicable if the building motion is not vigorous enough to change the flow field and wind load. However, the new generation of tall buildings today characterized by their slenderness and flexibility, which implies the importance of simultaneous modelling of wind flow and structural responses, namely “Aeroelastic” modelling. This type of computational fluid dynamics (CFD) analyses will reduce the uncertainty associated with the evaluation of wind-induced loads for flexible structures leading to a consequent reduction in the loads’ safety factor required for the structural design. However, the computational cost of the aeroelastic CFD analysis is expected to be higher than that of a rigid model CFD analysis due to the need of performing Finite element (FE) analysis within each time step of the CFD analysis to evaluate the structural response and its new shape at that specific time.

The current work proposes a workflow to perform aeroelastic simulation for a typical tall building examining different flexibility levels by changing the building stiffness, damping, and mass distribution. The study aims to examine the change in wind-induced load and response due to aeroelasticity. The Commonwealth Advisory Aeronautical Research Council (*CAARC*) building is considered, which was previously used by many researchers to calibrate and validate experimental (Melbourne 1980) and numerical (Bernardini et al. 2015; Elshaer et al. 2016a) studies.

2 PROPOSED FLUID STRUCTURE INTERACTION WORKFLOW

In order to conduct an aeroelastic CFD simulation, both the architectural and structural details of the structure need to be accurately modelled. In addition, the type of structural analysis needs to be properly selected knowing that this analysis will be repeatedly conducted within each time-step of the CFD transient simulation. Therefore, A simplified structural analysis scheme will lead to a considerable reduction in the computational time without affecting the accuracy of the developed wind loads and responses, since the structural model is only required to capture the motion of the structure. While a more sophisticated structural analysis can be conducted for computing the structural elements’ straining actions (i.e. wind forces and moments) and performing their structural design. Based on the previous discussion, it is proposed to develop an Equivalent Solid Model (*ESM*), which has structural dynamic properties similar to a target Skeletal Model (*SM*), including the mass distribution, stiffness, mode shapes, and damping. The process of matching the structural dynamic properties is conducted prior to the aeroelastic CFD simulation, as shown in Figure 1.

In order to match the mass distribution for the target *SM*, the total story load in the *ESM* will be uniformly redistributed over the story height, which can be performed by evaluating the equivalent density for the *ESM*, as per Equation 1. As for the structural damping, it can be matched by knowing the modal damping ratios and modal frequencies and evaluating the Rayleigh damping coefficients, as per Equation 2. Finally, the satisfaction of the stiffness and the fundamental mode shape can be achieved by conducting a structural analysis for the target *SM*, and evaluating the top story deflection under a triangular load that resembles wind load, as shown in Figure 2. After that Young’s modulus for the *ESM* can be evaluated, which develops a top story deflection similar to the target *SM* (Equation 3).

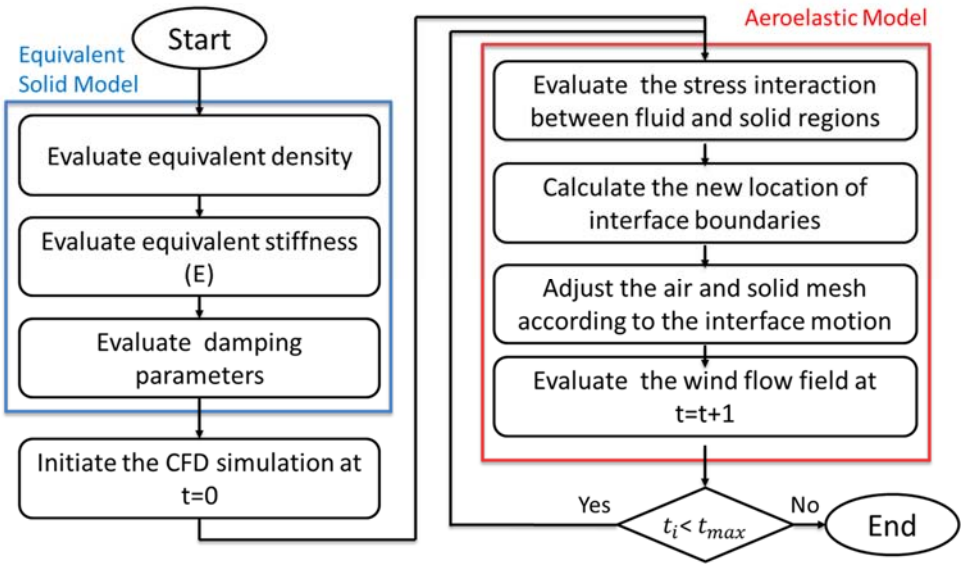

Figure 1 : Aeroelastic CFD simulation work flow

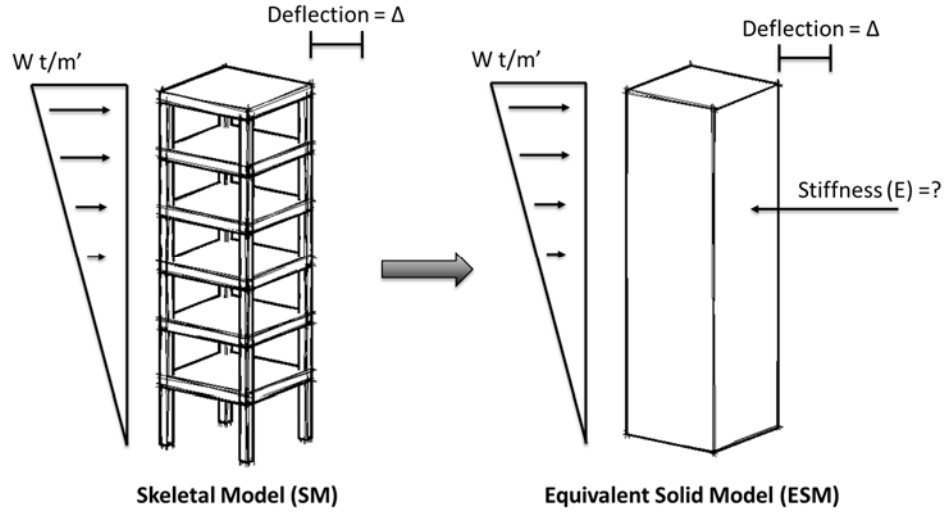

Figure 2 : Matching the stiffness of the Equivalent Solid Model (ESM) to that of the Skeletal Model (SM)

$$m_{ESM} = m_{SM} \quad \text{… (i)}$$

$$\rho_{ESM} = \frac{m_{SM}}{A_{story}.h_{story}} \quad \text{… (ii)}$$

Equation 1

Where m_{ESM} and m_{SM} are the mass of the *ESM* and *SM*, respectively, and ρ_{ESM}, A_{story} and h_{story} are the equivalent density, story area, and story height, respectively.

$$\tau_K = \frac{2\xi}{\omega_1+\omega_2} \quad \text{… (i)}$$

Equation 2

$$f_M = 2\xi\omega_1\left(1 - \frac{\omega_1}{\omega_1+\omega_2}\right) \quad \text{… (ii)}$$

Where τ_K and f_M are the mass of the Rayleigh damping coefficients, ω_1 and ω_2 are two reference vibration frequencies, and ξ is the damping ratio.

$$E_{ESM} = \frac{11}{120}\ \frac{w\,H^5}{u_{SM}\,I_{ESM}} \quad \text{… (i)}$$

Equation 3

Where E_{ESM} and I_{ESM} are Young's Modulus and moment of inertia the ESM, respectively, H is the height of the building, u_{SM} is the top story deflection evaluated from the SM, and w is the triangular distributed wind load applied to the tall building.

3 DESCRIPTION OF THE NUMERICAL MODEL AND CASE STUDIES

The current work adopts the CAARC building for defining the geometric details, as it has been a benchmark in several wind-related experimental and numerical studies. The building occupies a rectangular footprint (i.e. D=45 m. and B=30 m.) with a total height of 180 m. All the aerodynamic and structural characteristics are assigned in accordance with (Braun and Awruch 2009). Wind direction perpendicular to the wider side of the building is considered. The building is assumed to be a steel structure of natural frequency and damping ratio equal to 0.2 and 1%, respectively. The density, Young's Modulus and Poison's ratio of the ESM are assigned to be 160 Kg/m3, 230 MPa and 0.25, respectively. Full-scale aeroelastic LES models are utilized to simulate and assess tall buildings with different flexibility levels. The computational domain dimensions are defined based on the recommendations of (Franke et al. 2007) and (Dagnew and Bitsuamlak 2013), as shown in Figure 3. A no-slip wall boundary condition is assigned to the ground and all walls of the building, while symmetry plane boundary condition is assigned for top and side faces of the computational domain. The outflow of the computational domain is defined as a pressure outlet, while the inflow is defined as a smooth atmospheric boundary layer profile inlet (i.e. $v = v_{ref}z^{\alpha}$, $v_{ref} = 100\ m/sec.$, $\alpha = 0.19$).

The air computational domain is discretized into hexahedral meshes using the trimmer meshing algorithm for a total of 0.9M cells. The mesh size of 20 meters is selected for the region away from the study area at (Mesh Zone 1). The mesh resolution is further refined (i.e. mesh size = 3.0 meters) near the study building and in the region between the inlet and the building (Mesh Zone 3), as shown in Figure 4. The time step is chosen to be equals to 0.1 seconds maintaining Courant Number below 1.0 to ensure numerical convergence of the solver (Courant et al. 1928). The numerical simulations are conducted for 3,500 time-steps, which represent 350 seconds. The LES are conducted using (Star CCM+ v.10.02.011 2016) by employing a dynamic sub grid model proposed by (Smagorinsky 1963). As validation for the adopted CFD model, the results from Case 1 are compared to the experimental work presented by (Melbourne 1980) and the aeroelastic simulation by (Braun and Awruch 2009), as shown in Figure 5. The solid computational domain was discretized into 13K tetrahedral mesh cells. The structure is assumed to be made of a linear elastic material. A fluid-structure interaction interface is defined between the air and solid domain, where stresses are transferred to induce responses in both directions (from the air continuum to the solid one and vice-versa). A mesh morphing scheme is assigned to both meshing regions allowing the cells to skew according the induced motion of the interface (Figure 4).

As mentioned earlier the main target of this work is to examine the aeroelastic performance of tall buildings with different flexibility levels. This can be achieved by changing the stiffness, damping or the mass distribution of the structure. The parametric study includes 8 study cases, where Cases (1-4) are dedicated to examining different stiffness levels, Cases (1,5,6) examine different damping ratios, and Cases (1,7,8)

examine different ESM densities (changing the inertia forces by changing the mass of the structure). A summery of the study cases is presented in Table 1.

Table 1: Study cases description

Case	Young's Modulus (E in MPa)	Damping	Density (kg/m3)	Loading Scheme
Case 1	**230 (Eo)**	**No damping**	**160**	**No Ramping**
Case 2	2300 (10 Eo)	No damping	160	No Ramping
Case 3	115 (0.5 Eo)	No damping	160	No Ramping
Case 4	57.5 (0.25 Eo)	No damping	160	No Ramping
Case 5	230 (Eo)	0.50%	160	No Ramping
Case 6	230 (Eo)	1.00%	160	No Ramping
Case 7	230 (Eo)	No damping	100	No Ramping
Case 8	230 (Eo)	No damping	200	No Ramping

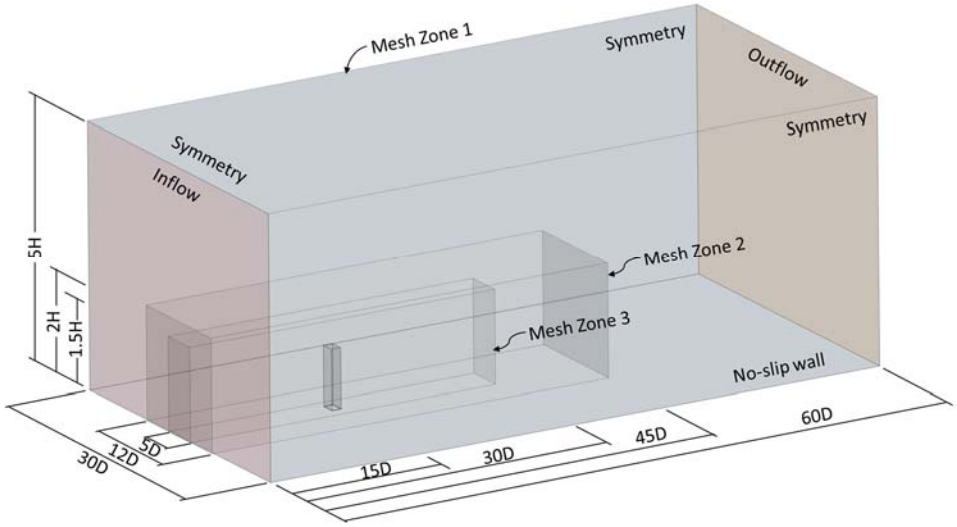

Figure 3 : Computational domain dimensions and boundary conditions

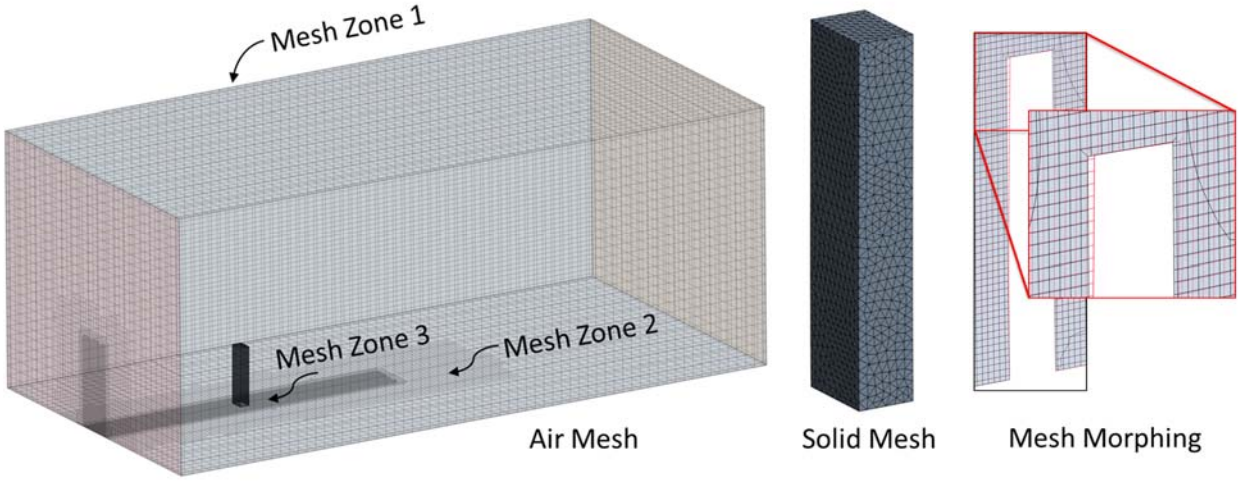

Figure 4 : Mesh grid resolution utilized in the aeroelastic CFD simulations for air and solid

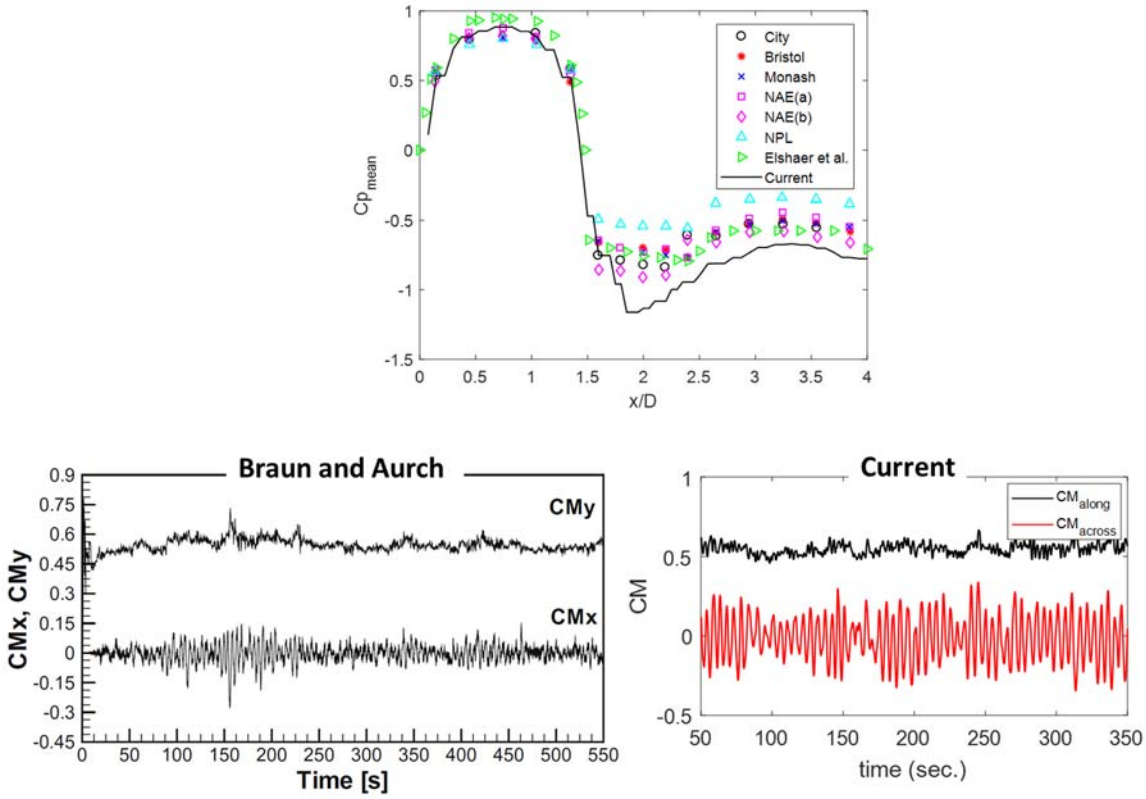

Figure 5 Validation of the aeroelastic CFD simulation

4 RESULTS AND DISCUSSIONS

Figure 6 shows the displacement contours developed by the building motion immersed in the wind flow. As shown in the figure, coupling the CFD with the FE analysis enabled the structure to vibrate and respond according to the loads induced by wind, which enhances the accuracy of CFD simulation for flexible structures. A parametric study is conducted by examining different stiffness, damping and mass distribution as shown in Figure 7, Figure 8, and Figure 9, respectively. The values of the mean pressure are found to decrease down to 7% with the increase in the building flexibility due to the dissipation of wind energy with the building motion. While the root-mean-square (rms) pressure values are found to increase up to 13% with the increase in building flexibility, which can be attributed to the additional turbulence cause by the building motion. Also, an excessive deflection is experienced by the building in the first 50 seconds of loading (transient period). While the across-wind deflection is found to be more sensitive to the natural frequency of the structure, which may match the vortex shedding frequency resulting in excessive lateral vibration (Case 3).

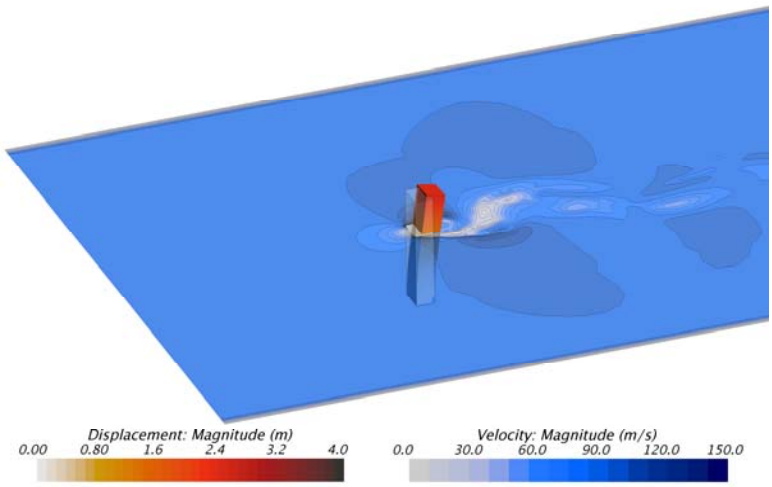

Figure 6 : Instantaneous wind velocity and building deflection (magnified by 10) contours

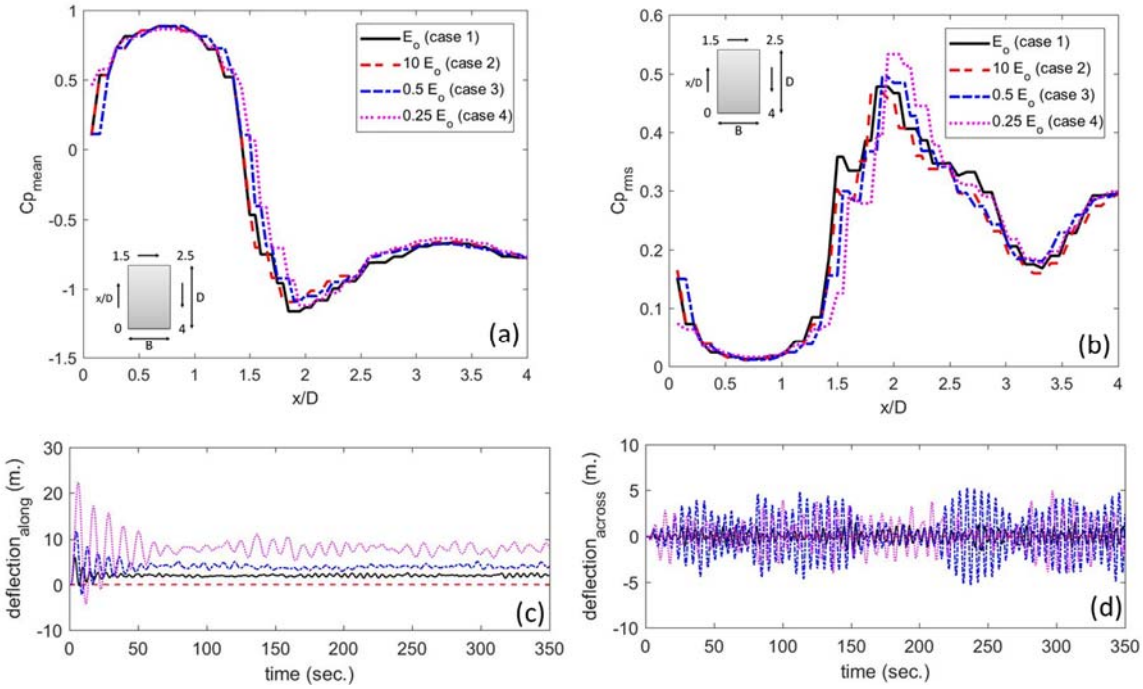

Figure 7 (a) mean and (b) rms distribution of Cp at 2H/3 of the building height; deflection time histories of the building top in the (c) along- and (d) across-wind directions (different stiffness, Cases 1-4)

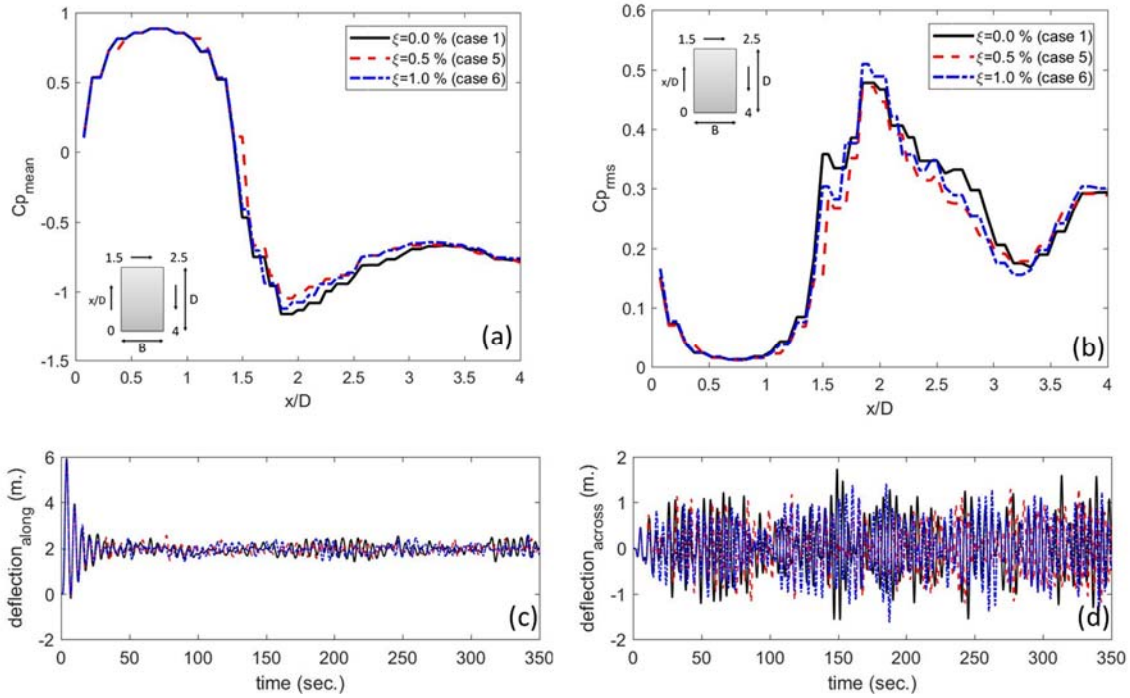

Figure 8 : (a) mean and (b) rms distribution of Cp at 2H/3 of the building height; deflection time histories of the building top in the (c) along- and (d) across-wind directions (different damping, Cases 1,5,6)

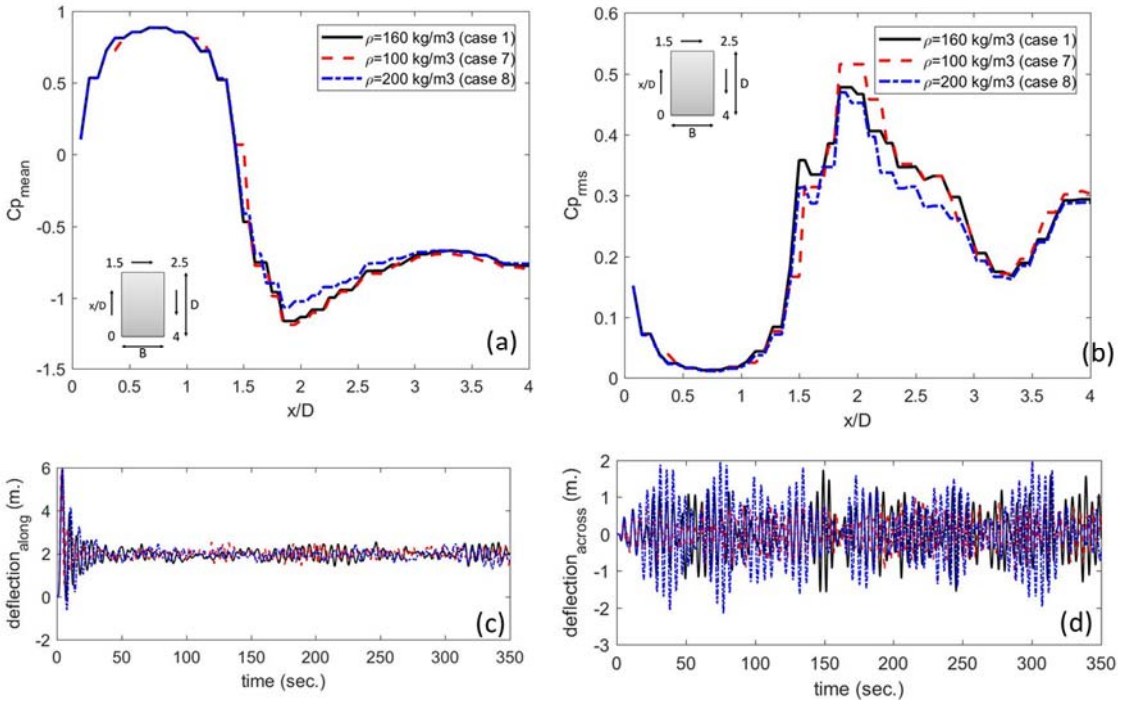

Figure 9 : (a) mean and (b) rms distribution of Cp at 2H/3 of the building height; deflection time histories of the building top in the (c) along- and (d) across-wind directions (different denisties, Cases 1,7,8)

5 CONCLUSION

A workflow is developed for conducting aeroelastic Computational Fluid Dynamics (CFD) simulation by augmenting Finite element analysis to the CFD simulation. The proposed workflow is examined for a typical tall building immersed in wind flow. The study presents a parametric study to explore different flexibility ranges by changing the stiffness, damping and mass distribution of the structure. Within the adopted flexibility levels, the structure is found to experience up to 7% decrease in the mean wind pressure and 13% increase in the fluctuating wind pressure. The building top deflection in the along-wind is significantly affected by the building flexibility, while the across-wind deflection is more sensitive to the change in building stiffness due to the consequent change in the building natural frequency. This change in building frequency may resonate the shedding frequency with the building natural frequency leading to an excessive motion. In future research, it is planned to examine the proposed workflow while immersing the structure in a turbulent flow, and to assess the deflection and serviceability consideration for human comfort. Also, it is planned to expand the process of developing the equivalent solid model to match wider range of structural properties.

Acknowledgements

The authors would like to acknowledge the financial support from Ontario Center of Excellence (OCE), National Science and Engineering Research Center (NSERC), the Southern Ontario Smart Computing Innovation Platform (SOSCIP), and Canada Research Chair. The authors are grateful for access to SciNet and SHARCNET, and for the support received from their excellent technical staff.

References

Aboshosha, H., Elshaer, A., Bitsuamlak, G., and El Damatty, A. (2015). “Consistent inflow turbulence generator for LES evaluation of wind-induced responses for tall buildings.” *Journal of Wind Engineering and Industrial Aerodynamics*, 142(JULY), 198–216.

Adamek, K., Vasan, N., Elshaer, A., English, E., and Bitsuamlak, G. (2017). “Pedestrian level wind assessment through city development: A study of the financial district in Toronto.” *Sustainable Cities and Society*, 35.

Bernardini, E., Spence, S. M. J., Wei, D., and Kareem, A. (2015). “Aerodynamic shape optimization of civil structures: A CFD-enabled Kriging-based approach.” *Journal of Wind Engineering and Industrial Aerodynamics*, Elsevier, 144, 154–164.

Bitsuamlak, G. T., Dagnew, A. K., and Erwin, J. (2010). “Evaluation of wind loads on solar panel modules using CFD.” *The Fifth International Symposium on Computational Wind Engineering, Chapel Hill, North Carolina, USA, May*, 23–27.

Blocken, B. J. E., and Stathopoulos, T. (2013). “CFD simulation of pedestrian-level wind conditions around buildings: Past achievements and prospects.”

Braun, A. L., and Awruch, A. M. (2009). “Aerodynamic and aeroelastic analyses on the CAARC standard tall building model using numerical simulation.” *Computers & Structures*, Elsevier, 87(9), 564–581.

Catalina, T., Virgone, J., and Kuznik, F. (2009). “Evaluation of thermal comfort using combined CFD and experimentation study in a test room equipped with a cooling ceiling.” *Building and Environment*, Elsevier, 44(8), 1740–1750.

Chu, a K. M., Kwok, R. C. W., and Yu, K. N. (2005). “Study of pollution dispersion in urban areas using Computational Fluid Dynamics (CFD) and Geographic Information System (GIS).” *Environmental Modelling & Software*, 20(3), 273–277.

Courant, R., Friedrichs, K., and Lewy, H. (1928). “Über die partiellen Differenzengleichungen der mathematischen Physik.” *Mathematische annalen*, Springer, 100(1), 32–74.

Dagnew, A., and Bitsuamlak, G. T. (2013). “Computational evaluation of wind loads on buildings: a review.” *Wind Struct*, 16(6), 629–660.

Dagnew, A. K., and Bitsuamlak, G. T. (2014). “Computational evaluation of wind loads on a standard tall building using LES.” *Wind and Structures*, 18(5), 567–598.

Dagnew, G. B., and Bitsuamlak, G. T. (2012). “Large eddy simulation for wind-induced response of tall buildings located in a city center.” *The 2012 Engineering Mechanics Institute & 11th ASCE Joint Specialty Conference on Probabilistic Mechanics and Structural Reliability (EMI/PMC 2012)*, 17–20.

Ding, W., Hasemi, Y., and Yamada, T. (2005). “Natural ventilation performance of a double-skin façade with a solar chimney.” *Energy and Buildings*, Elsevier, 37(4), 411–418.

Elshaer, A., Aboshosha, H., Bitsuamlak, G., El Damatty, A., and Dagnew, A. (2016a). “LES evaluation of wind-induced responses for an isolated and a surrounded tall building.” *Engineering Structures*, Elsevier, 115, 179–195.

Elshaer, A., Bitsuamlak, G., and El Damatty, A. (2016b). “Enhancing wind performance of tall buildings using corner aerodynamic optimization.” *Engineering Structures*.

Elshaer, A., Gairola, A., Adamek, K., and Bitsuamlak, G. (2017). “Variations in wind load on tall buildings due to urban development.” *Sustainable Cities and Society*, 34.

Franke, J., Hellsten, A., Schlünzen, H., and Carissimo, B. (2007). “Best Practice Guideline for the CFD Simulation of Flows in the Urban Environment. COST Action 732: Quality Assurance and Improvement of Microscale Meteorological Models.” *Hamburg, Germany*.

Gousseau, P., Blocken, B., Stathopoulos, T., and van Heijst, G. J. F. (2011). “CFD simulation of near-field pollutant dispersion on a high-resolution grid: A case study by LES and RANS for a building group in downtown Montreal.” *Atmospheric Environment*, 45(2), 428–438.

Hajra, B., Bitsuamlak, G. T., Aboshosha, H., and Elshaer, A. (2016). “Large eddy simulation of wind induced loads on a low rise building with complex roof geometry.” *Proceedings, Annual Conference - Canadian Society for Civil Engineering*.

van Hooff, T., Blocken, B., Aanen, L., and Bronsema, B. (2011). “A venturi-shaped roof for wind-induced natural ventilation of buildings: wind tunnel and CFD evaluation of different design configurations.” *Building and Environment*, Elsevier, 46(9), 1797–1807.

Lee, S., Lee, J. S., and Kim, J. D. (1997). “Prediction of vortex-induced wind loading on long-span bridges.” *Journal of Wind Engineering and Industrial Aerodynamics*, Elsevier, 67, 267–278.

Melbourne, W. H. (1980). “Comparison of measurements on the CAARC standard tall building model in simulated model wind flows.” *Journal of Wind Engineering and Industrial Aerodynamics*, Elsevier, 6(1–2), 73–88.

Montazeri, H., and Blocken, B. (2013). “CFD simulation of wind-induced pressure coefficients on buildings with and without balconies: validation and sensitivity analysis.” *Building and Environment*, Elsevier, 60, 137–149.

Pospisil, J., Katolicky, J., and Jicha, M. (2004). “A comparison of measurements and CFD model predictions for pollutant dispersion in cities.” *Science of The Total Environment*, 334, 185–195.

Smagorinsky, J. (1963). *General circulation experiments with the primitive equations*.

Star CCM+ v.10.02.011. (2016). “CD-ADAPCO product. <www.cd-adapco.com/products/star-ccm>.” CD-ADAPCO Product.

Tablada, A., De Troyer, F., Blocken, B., Carmeliet, J., and Verschure, H. (2009). “On natural ventilation and thermal comfort in compact urban environments–the Old Havana case.” *Building and Environment*, Elsevier, 44(9), 1943–1958.

Yang, W., Quan, Y., Jin, X., Tamura, Y., and Gu, M. (2008). “Influences of equilibrium atmosphere boundary layer and turbulence parameter on wind loads of low-rise buildings.” *Journal of wind engineering and industrial aerodynamics*, Elsevier, 96(10), 2080–2092.